Inorg. Chem. **2007**, *46*, 10892–10900

Syntheses, Structures, and Sensitized Lanthanide Luminescence by Pt → Ln (Ln = Eu, Nd, Yb) Energy Transfer for Heteronuclear $PtLn_2$ and Pt_2Ln_4 Complexes with a Terpyridyl-Functionalized Alkynyl Ligand

Xiu-Ling Li,[†,‡] Lin-Xi Shi,[†] Li-Yi Zhang,[†] Hui-Min Wen,[†] and Zhong-Ning Chen*[,†]

State Key Laboratory of Structural Chemistry, Fujian Institute of Research on the Structure of Matter, Chinese Academy of Sciences, Fuzhou, Fujian 350002, China, and School of Chemistry and Chemical Engineering, Xuzhou Normal University, Xuzhou, Jiangsu 221116, China

Received August 7, 2007

Reaction of Pt(dppm-*P*,*P*′)Cl_2 (dppm = 1,2-bis(diphenylphosphino)methane) with HC≡CPhtpy (HC≡CPhtpy = 4′-(4-ethynylphenyl)-2,2′:6′,2″-terpyridine) in the presence of copper(I) iodide and diisopropylamine induced isolation of mononuclear complex c*is*-Pt(dppm-*P*,*P*′)(C≡CPhtpy)$_2$ (**1**), which can be converted into face-to-face diplatinum(II) species $Pt_2(\mu$-dppm$)_2$(C≡CPhtpy)$_4$ (**5**) when equivalent dppm is added. Incorporating **1** or **5** to Ln(hfac)$_3$(H_2O)$_2$ (Hhfac = hexafluoroacetylacetone) gave $PtLn_2$ (Ln = Nd (**2**), Eu (**3**), Yb (**4**)) or Pt_2Ln_4 (Ln = Nd (**6**), Eu (**7**), Gd (**8**), Yb (**9**)) adducts with the lanthanide centers chelated by terdentate terpyridyl in the bridging C≡CPhtpy. The structures of **1**, **6**, **7**, and **9** were determined by X-ray crystallography. Upon excitation at λ_{ex} = 360–450 nm (**2**–**4**) or 360–500 nm (**6**–**9**), where the Pt^{II} alkynyl antenna chromophores absorb strongly but the model complexes Ln(hfac)$_3$(HC≡CPhtpy) lack obvious absorption in this region, these $PtLn_2$ and Pt_2Ln_4 (Ln = Nd, Eu, Yb) species exhibit bandlike lanthanide luminescence that is typical of the corresponding Ln^{3+} ions, demonstrating unambiguously that efficient Pt → Ln energy transfer occurs indeed from the Pt^{II} alkynyl antenna chromophores to the lanthanide centers across the bridging C≡CPhtpy with intramolecular Pt···Ln distances being ca. 14.2 Å. The Pt → Ln energy transfer rate (k_{ET}) is 6.07×10^7 s^{-1} for Pt_2Nd_4 (**6**) and 2.12×10^5 s^{-1} for Pt_2Yb_4 (**9**) species.

Introduction

Recent interests in near-infrared (NIR) luminescence of lanthanide(III) complexes have been significantly stimulated by their extensive applications in the fields including light-emitting diodes, optical communication, magnetic resonance imaging, laser and biological assay, etc.[1−3] Because of the extremely weak absorption from f−f transitions for the Ln^{III} ions, luminescence from lanthanides is usually sensitized by organic antenna chromophores which absorb strongly in the UV−vis region.[1−3] Using d-block metal chromophores as energy donors to sensitize near-infrared lanthanide luminescence is a recently developed approach,[4,5] initiated by van Veggel et al.[4] at the beginning of this century and developed later by others.[5−16] Compared with purely organic chromophores, the d-block metallorganic sensitizers afford a series of advantages,[5] including the broad absorption spanning the visible region induced by the red-shifted ILCT

* To whom correspondence should be addressed. E-mail: czn@fjirsm.ac.cn.
† Fujian Institute of Research on the Structure of Matter.
‡ Xuzhou Normal University.

(1) Comby S.; Bünzli, J.-C. G. *Handbook on the Physics and Chemistry of Rare Earths*; Elsevier BV: Amsterdam, 2007; Chapter 235, Vol. 37.
(2) (a) Bünzli, J.-C. G.; Piguet, C. *Chem. Soc. Rev.* **2005**, *34*, 1048. (b) Bünzli, J.-C. G. *Acc. Chem. Res.* **2006**, *39*, 53. (c) Bünzli, J.-C. G.; Piguet, C. *Chem. Rev.* **2002**, *102*, 1897.
(3) (a) Petoud, S.; Cohen, S. M.; Bünzli, J.-C. G.; Raymond, K. N. *J. Am. Chem. Soc.* **2003**, *125*, 13324. (b) Petoud, S.; Muller, G.; Moore, E. G.; Xu, J.; Sokolnicki, J.; Riehl, J. P.; Le, U. N.; Cohen, S. M.; Raymond, K. N. *J. Am. Chem. Soc.* **2007**, *129*, 77. (c) Zhang, J, Badger, P. D.; Geib, S. J.; Petoud, S. *Angew. Chem., Int. Ed.* **2005**, *44*, 2508. (d) Quici, S.; Cavazzini, M.; Marzanni, G.; Accorsi, G.; Armaroli, N.; Ventura, B.; Barigelletti, F. *Inorg. Chem.* **2005**, *44*, 529. (e) Yang, X.-P.; Jones, R. A. *J. Am. Chem. Soc.* **2005**, *127*, 7686.
(4) Klink,S. I.; Keizer, van Veggle, H.; F. C. J. M. *Angew. Chem., Int. Ed.* **2000**, *39*, 4319.
(5) (a) Ward, M. D. *Coord. Chem. Rev.* **2007**, *251*, 1663. (b) Shavaleev, N. M.; Moorcraft, L. P.; Pope, S. J. A.; Bell, Z. R.; Faulkner, S.; Ward, M. D. *Chem. Commun.* **2003**, 1134. (c) Shavaleev, N. M.; Moorcraft, L. P.; Pope, S. J. A.; Bell, Z. R.; Faulkner, S.; Ward, M. D. *Chem.—Eur. J.* **2003**, *9*, 5283. (d) Shavaleev, N. M.; Accorsi, G.; Virgili, D.; Bell, Z. R.; Lazarides, T.; Calogero, G.; Armaroli, N.; Ward, M. D. *Inorg. Chem.* **2005**, *44*, 61. (e) Davies, G. M.; Pope, S. J. A.; Adams, H.; Faulkner, S.; Ward, M. D. *Inorg. Chem.* **2005**, *44*, 4656. (f) Herrera, J. M.; Pope, S. J. A.; Adams, H.; Faulkner, S.; Ward, M. D. *Inorg. Chem.* **2006**, *45*, 3895. (g) Herrera, J. M.; Ward, M. D.; Adams, H.; Pope, S. J. A.; Faulkner, S. *Chem. Commun.* **2006**, 1851. (h) Kennedy, F.; Shavaleev, N. M.; Koullourou, T.; Bell, Z. R.; Jeffery, J. C.; Faulkner, S.; Ward, M. D. *Dalton Trans.* **2007**, 1492.

10.1021/ic7015676 CCC: $37.00
Published on Web 11/14/2007

(intraligand charger transfer) or MLCT (metal-to-ligand charge transfer) transitions, relatively high triplet quantum yields due to the rapid intersystem crossing arising from the heavy metal effect, and relatively long-lived triplet excited states that facilitate energy transfer to the adjacent Ln^{III} centers. A key step for fabrication of transition metal and lanthanide heteronuclear (d−f) arrays is to design suitable bridging connectors that can promote the energy transfer from the d-block antenna chromophores to the lanthanide centers. Apparently, the absence of a conjugated pathway between energy donor and acceptor is unfavorable for energy-transfer via a double electron exchange (Dexter) process and, hence, retards energy-transfer rates.[4,7] By this consideration, judicious selection of bifunctional bridging ligands with favorable π-conjugation is vital to effective energy transfer from the d-block organometallic chromophores so as to achieve long-lived NIR lanthanide luminescence with high efficicency.[5,15,16] A series of oligopyridine-functionalized alkynyl ligands with favorable conjugation have been utilized for the construction of d-block chromophores and subsequent d-f arrays in recent years,[15−17] in which the "soft" donors such as C, N, P, and S atoms are bound to the transition metal ions and the "hard" donors such as O and N atoms are associated with the lanthanide centers.

It has been demonstrated that reactions of *cis*-Pt(dppe)Cl_2 (dppe = 1,2-bis(diphenylphosphino)ethane) or *cis*-Pt(dppp)Cl_2 (dppp = 1,3-bis(diphenylphosphino)propane) with alkynyl ligands HC≡CR give unexceptionally *cis*-Pt(dppe)$(C{\equiv}CR)_2$ or *cis*-Pt(dppp)$(C{\equiv}CR)_2$ (R = alkyl or aryl).[17−19] In contrast, the reactions using *cis*-Pt(dppm-*P*,*P*′)Cl_2 (dppm = bis(diphenylphosphino)methane) instead of *cis*-Pt(dppe)Cl_2 or *cis*-Pt(dppp)Cl_2 always induce isolation of the diplatinum(II) species $Pt_2(\mu\text{-dppm})_2(C{\equiv}CR)_4$ with the two Pt^{II} coordination planes face-to-face arranged,[15,20,21] in which the two Pt^{II} centers are linked by two dppm to afford a $Pt_2P_4C_2$ eight-membered ring. The dppm-chelated mononuclear Pt^{II} species *cis*-Pt(dppm-*P*,*P*′)$(C{\equiv}CR)_2$ similar structurally to the counterparts *cis*-Pt(dppe)$(C{\equiv}CR)_2$ or *cis*-Pt(dppp)$(C{\equiv}CR)_2$, however, have never been reported before. During our recent studies on the reactions of Pt(dppm-*P*,*P*′)Cl_2 with terpyridyl-functionalized alkynyl ligand 4′-(4-ethynylphenyl)-2,2′:6′,2″-terpyridine (HC≡CPhtpy), the mononuclear complex *cis*-Pt(dppm-*P*,*P*′)$(C{\equiv}CPhtpy)_2$ (**1**) containing chelating dppm was successfully isolated for this first time. Moreover, **1** can be transformed into the face-to-face diplatinum(II) species $Pt_2(\mu\text{-dppm})_2(C{\equiv}CPhtpy)_4$ (**5**) in the presence of equimolar dppm. Both **1** and **5** exhibit intense, long-lived room-temperature phosphorescence which qualifies them as favorable energy donors to achieve sensitized lanthanide luminescence in the Pt−Ln heteronuclear complexes by effective Pt → Ln energy transfer. This article describes the preparation, characterization, and photophysical properties of **1** and **5** and their $Ln(hfac)_3$ (Hhfac = hexafluoroacetylacetone) adducts *cis*-Pt(dppm-*P*,*P*′)$(C{\equiv}CPhtpy)_2\{Ln(hfac)_3\}_2$ (Ln = Nd (**2**), Eu (**3**), Yb (**4**)) and $Pt_2(\mu\text{-dppm})_2(C{\equiv}CPhtpy)_4\{Ln(hfac)_3\}_4$ (Ln = Nd (**6**), Eu (**7**), Gd (**8**), Yb (**9**)).

Experimental Section

Materials and Reagents. All operations were carried out under dry argon atmosphere by using Schlenk techniques at ambient temperature and a vacuum-line system unless specified. The solvents were dried, distilled, and degassed prior to use except those for spectroscopic measurements were of spectroscopic grade. Bis(diphenylphosphino)methane (dppm) was obtained from Acros. 4′-(4-Ethynylphenyl)-2,2′:6′,2″-terpyridine (HC≡Cphtpy), *cis*-Pt(dppm-*P*,*P*′)Cl_2, and $Ln(hfac)_3(H_2O)_2$ were prepared by the literature methods.[22,23]

***cis*-Pt(dppm-*P*,*P*′)$(C{\equiv}CPhtpy)_2$ (1).** *cis*-Pt(dppm-*P*,*P*′)Cl_2 (136.8 mg, 0.21 mmol), CuI (6.5 mg, 0.034 mmol), and diisopropylamine (2.5 mL) were added successively to a dichloromethane−methanol (8:3 v/v, 55 mL) solution of HC≡CPhtpy (159.9 mg, 0.48 mmol).

(6) (a) Imbert, D.; Cantuel, M.; Bünzli, J.-C. G.; Bernardinelli, G.; Piguet, C. *J. Am. Chem. Soc*. **2003**, *125*, 15698. (b) Torelli, S.; Imbert, D.; Cantuel, M.; Delahaye, S.; Hauser, A.; Bünzli, J.-C. G.; Piguet, C. *Chem.−Eur. J*. **2005**, *11*, 3228. (c) Torelli, S.; Delahaye, S.; Hauser, A.; Bernardinelli, G.; Piguet, C. *Chem.−Eur. J*. **2004**, *10*, 3503. (d) Cantuel, M.; Gumy, F.; Bünzli, J. C. G.; Piguet, C. *Dalton Trans*. **2006**, 2647.

(7) (a) Pope, S. J. A.; Coe, B. J.; Faulkner, S.; Bichenkova, E. V.; Yu, X.; Douglas, K. T. *J. Am. Chem. Soc*. **2004**, *126*, 9490. (b) Pope, S. J. A.; Coe, B. J; Faulkner, S.; Laye, R. H. *Dalton Trans*. **2005**, 1482. (c) Pope, S. J. A.; Coe, B. J.; Faulkner, S. *Chem. Commun*. **2004**, 1550. (d) Sénéchal-David, K.; Pope, S. J. A.; Quinn, S.; Faulkner, S.; Gunnlaugsson, T. *Inorg. Chem*. **2006**, *45*, 10040.

(8) Coppo, P.; Duati, M.; Kozhevnikov, V. N.; Hofstraat, J. W.; De Cola, L. *Angew. Chem., Int. Ed*. **2005**, *44*, 1806.

(9) Guo, D.; Duan, C.-Y.; Lu, F.; Hasegawa, Y.; Meng, Q.-J.; Yanagida, S. *Chem. Commun*. **2004**, 1486.

(10) Rawashdeh-Omary, M. A.; Larochelle, C. L.; Patterson, H. H. *Inorg. Chem*. **2000**, *39*, 4527.

(11) Beeby, A.; Dickins, R. S.; FitzGerald, S.; Govenlock, L. J.; Maupin, C. L.; Parker, D.; Riehl, J. P.; Siligardi, G.; Williams, J. A. G. *Chem. Commun*. **2000**, 1183.

(12) Glover, P. B.; Ashton, P. R.; Childs, L. J.; Rodger, A.; Kercher, M.; Williams, R. M.; De Cola, L.; Pikramenou, Z. *J. Am. Chem. Soc*. **2003**, *125*, 9918.

(13) (a) Beer, P. D.; Szemes, F.; Passaniti, P.; Maestri, M. *Inorg. Chem*. **2004**, *43*, 3965. (d) Sambrook, M. R.; Curiel, D.; Hayes, E. J.; Beer, P. D.; Pope, S. J. A.; Faulkner, S. *New J. Chem*. **2006**, *30*, 1133.

(14) Sanada, T.; Suzuki, T.; Yoshida, T.; Kaizaki, S. *Inorg. Chem*. **1998**, *37*, 4712.

(15) (a) Xu, H.-B.; Zhang, L.-Y.; Xie, Z.-L.; Ma, E.; Chen, Z.-N. *Chem. Commun*. **2007**, 2744. (b) Xu, H.-B.; Shi, L.-X.; Ma, E.; Zhang, L.-Y.; Wei, Q.-H.; Chen, Z.-N. *Chem. Commun*. **2006**, 1601.

(16) Ronson, T. K.; Lazarides, T.; Adams, H.; Pope, S. J. A.; Sykes, D.; Faulkner, S.; Coles, S. J.; Hursthouse, M. B.; Clegg, W.; Harrington, R. W.; Ward, M. D. *Chem.−Eur. J*. **2006**, *12*, 9299.

(17) Li, X.-L.; Dai, F.-R.; Zhang, L.-Y.; Zhu, Y.-M.; Peng, Q.; Chen, Z.-N. *Organometallics* **2007**, *26*, 4483.

(18) (a) Bruce, M. I.; Costuas, K.; Halet, J.-F.; Hall, B. C.; Low, P. J.; Nicholson, B. K.; Skelton, B. W.; White, A. H. *J. Chem. Soc., Dalton Trans*. **2002**, 383. (b) Saha, R.; Qaium, Md. A.; Debnath, D.; Younus, M.; Chawdhury, N.; Sultana, N.; Kociok-Köhn, G.; Ooi, L.; Raithby, P. R.; Kijima, M. *Dalton Trans*. **2005**, 2760. (c) Yamazaki, S.; Deeming, A. J. *J. Chem. Soc., Dalton Trans*. **1993**, 3051. (d) Long, N. J.; Wong, C. K.; White, A. J. P. *Organometallics* **2006**, *25*, 2525.

(19) Janka, M.; Anderson, G. K.; Rath, N. P. *Organometallics* **2004**, *23*, 4382.

(20) (a) Langrick, C. R.; McEwan, D. M.; Pringle, P. G.; Shaw, B. L. *J. Chem. Soc., Dalton Trans*. **1983**, 2487. (b) Pringle, P. G.; Shaw, B. L. *J. Chem. Soc., Chem. Commun*. **1982**, 581.

(21) (a) Yam, V. W.-W.; Yu, K.-L.; Wong, K. M.-C.; Cheung, K.-K. *Organometallics* **2001**, *20*, 721. (b) Yam, V. W.-W.; Hui, C.-K.; Wong, K. M.-C.; Zhu, N.; Cheung, K.-K. *Organometallics* **2002**, *21*, 4326. (c) Hui, C.-K.; Chu, B. W.-K.; Zhu, N.; Yam, V. W.-W. *Inorg. Chem*. **2002**, *41*, 6178. (d) Wong, K. M.-C.; Hui, C.-K.; Yu, K.-L.; Yam, V. W.-W. *Coord. Chem. Rev*. **2002**, *229*, 123.

(22) Grosshenny, V.; Romero, F. M.; Ziessel, R. *J. Org. Chem*. **1997**, *62*, 1491.

(23) (a) Brown, M. P.; Puddephatt, R. J.; Rashidi, M.; Seddon, K. R. *J. Chem. Soc., Dalton Trans*. **1977**, 951. (b) Hasegawa, Y.; Kimura, Y.; Murakoshi, K.; Wada, Y.; Kim, J.-H.; Nakashima, N.; Yamanaka, T.; Yanagida, S. *J. Phys. Chem*. **1996**, *100*, 10201.

Table 1. Crystallographic Data for **1**·2CH_2Cl_2·H_2O, **6**, **7**, and **9**·2CH_2Cl_2

param	**1**·2CH_2Cl_2·H_2O	**6**	**7**	**9**·2CH_2Cl_2
formula	$C_{73}H_{56}Cl_4N_6OP_2Pt$	$C_{202}H_{112}F_{72}N_{12}Nd_4O_{24}P_4Pt_2$	$C_{202}H_{112}Eu_4F_{72}N_{12}O_{24}P_4Pt_2$	$C_{204}H_{116}Cl_4F_{72}N_{12}O_{24}P_4Pt_2Yb_4$
fw	1432.0	5550.06	5580.94	5835.11
temp, K	293(2)	293(2)	293(2)	293(2)
space group	*C*2/*c*	$P\bar{1}$	$P2_1/c$	$P2_1/c$
a, Å	17.585(5)	15.409(3)	21.161(6)	21.113(11)
b, Å	19.639(5)	18.761(4)	34.020(8)	33.841(17)
c, Å	20.230(5)	25.654(5)	19.924(5)	19.906(10)
α, deg		75.785(7)		
β, deg	110.934(4)	76.278(6)	103.690(5)	104.437(6)
γ, deg		75.276(7)		
V, Å^3	6525(3)	6831(2)	13 936(6)	13 773(12)
Z	4	1	2	2
ρ_{calcd}, g/cm^{-3}	1.458	1.349	1.330	1.407
μ, mm^{-1}	2.413	1.891	2.009	2.519
radiation (λ, Å)	0.710 73	0.710 73	0.710 73	0.710 73
R1[a]	0.0372	0.0711	0.0746	0.0623
wR2[b]	0.0965	0.2094	0.1850	0.1614
GOF	1.095	1.055	1.047	1.050

[a] $R1 = \Sigma|F_o - F_c|/\Sigma F_o$. [b] $wR2 = \Sigma[w(F_o^2 - F_c^2)^2]/\Sigma[w(F_o^2)]^{1/2}$.

The mixture was stirred at ambient temperature with exclusion of light for 1 week, producing a pale yellow precipitate. After filtration, the pale yellow solid was washed thrice with 5 mL of dichloromethane and dried in vacuo. The product is an air-stable, pale-yellow crystalline solid. Yield: 69% (185 mg). Anal. Calcd for $C_{71}H_{50}N_6P_2Pt{\cdot}CH_2Cl_2$: C, 65.06; H, 3.94; N, 6.32. Found: C, 65.62; H, 3.98; N, 6.22. ES-MS (*m*/*z*): 1245.2, $[M + H]^+$. IR (KBr, cm^{-1}): ν 2106 s (C≡C).

***cis*-{Pt(dppm-*P*,*P*′)(C≡CPhtpy)$_2$}{Ln(hfac)$_3$}$_2$ (Ln = Nd (2), Eu (3), Yb (4)).** These complexes were prepared by reactions of **1** with 2.5 equiv of Ln(hfac)$_3$(H_2O)$_2$ in dichloromethane with stirring for 0.5 h at room temperature. After filtration, the solutions were concentrated to precipitate the greenish-yellow or yellow products by addition of *n*-hexane. Layering *n*-hexane onto the concentrated dichloromethane solutions in the absence of light gave the products as yellow prism crystals in a few days.

2. Yield: 87%. Anal. Calcd for $C_{101}H_{56}F_{36}N_6Nd_2O_{12}P_2Pt$: C, 43.72; H, 2.03; N, 3.03. Found: C, 44.10; H, 2.13; N, 2.92. IR (KBr, cm^{-1}): ν 2109 m (C≡C), 1652 s (C═O).

3. Yield: 90%. Anal. Calcd for $C_{101}H_{56}Eu_2F_{36}N_6O_{12}P_2Pt$: C, 43.47; H, 2.02; N, 3.01. Found: C, 43.55; H, 2.10; N, 2.95. IR (KBr, cm^{-1}): ν 2109 m (C≡C), 1654 s (C═O).

4. Yield: 92%. Anal. Calcd for $C_{101}H_{56}F_{36}N_6O_{12}P_2PtYb_2{\cdot}CH_2Cl_2$: C, 41.99; H, 2.00; N, 2.88. Found: C, 42.27; H, 2.10; N, 2.85. IR (KBr, cm^{-1}): ν 2107 m (C≡C), 1658 s (C═O).

Pt$_2$(μ-dppm)$_2$(C≡CPhtpy)$_4$ (5). Method A. dppm (15.9 mg, 0.041 mmol) was added to a suspension solution of **1** (50.6 mg, 0.041 mmol) in dichloromethane (10 mL). After stirring of the mixture at room temperature for 5 d in the absence of light, the resulting precipitate was filtered off and washed thrice with 10 mL of dichloromethane to give **5** as an air-stable, yellow crystalline solid. Yield: 59% (30 mg). Anal. Calcd for $C_{142}H_{100}N_{12}P_4Pt_2$: C, 68.54; H, 4.05; N, 6.75. Found: C, 68.60; H, 4.30; N, 6.57. ES-MS (*m*/*z*): 2487.2, $[M + H]^+$; 1244.4, $[M - Pt(dppm)(C{\equiv}Cphtpy)_2 + H]^+$. IR (KBr, cm^{-1}): ν 2102 s (C≡C).

Method B. Pt(dppm-*P*,*P*′)Cl_2 (72.7 mg, 0.11 mmol), CuI (2.3 mg, 0.012 mmol), and diisopropylamine (2.5 mL) were added successively to a dichloromethane (60 mL) solution of HC≡CPhtpy (89.9 mg, 0.27 mmol) in the presence of dppm (43.1 mg, 0.11 mmol). After the mixture was stirred at room temperature with exclusion of light for 5 d, a little yellow solid precipitated from the mixture. After filtration, the yellow solid was washed thrice with 10 mL of dichloromethane to give **5** as yellow crystalline solid. Yield: 10% (15 mg).

{Pt$_2$(μ-dppm)$_2$(C≡CPhtpy)$_4$}{Ln(hfac)$_3$}$_4$ (Ln = Nd (6), Eu (7), Gd (8), Yb (9)). Synthetic procedures of **6**−**9** are similar to those of **2**−**4** with a slight modification. To a dichloromethane solution of **5** was added 4.5 equiv of Ln(hfac)$_3$(H_2O)$_2$ with stirring for 0.5 h at room temperature, giving a clear yellow to orange solution. Layering *n*-hexane onto the concentrated dichloromethane solutions gave the desired complexes as orange yellow or orange prismatic crystals in the absence of light.

6. Yield: 40%. Anal. Calcd for $C_{202}H_{112}F_{72}N_{12}Nd_4O_{24}P_4Pt_2$: C, 43.72; H, 2.03; N, 3.03. Found: C, 43.90; H, 2.21; N, 2.95. IR (KBr, cm^{-1}): ν 2098 m (C≡C), 1653 s (C═O).

7. Yield: 45%. Anal. Calcd for $C_{202}H_{112}Eu_4F_{72}N_{12}O_{24}P_4Pt_2$: C, 43.47; H, 2.02; N, 3.01. Found: C, 43.60; H, 2.18; N, 2.95. IR (KBr, cm^{-1}): ν 2098 m (C≡C), 1655 s (C═O).

8. Yield: 43%. Anal. Calcd for $C_{202}H_{112}F_{72}N_{12}O_{24}P_4Pt_2Gd_4$: C, 43.31; H, 2.02; N, 3.00. Found: C, 43.06; H, 2.10; N, 2.92. IR (KBr, cm^{-1}): ν 2098 m (C≡C), 1657 s (C═O).

9. Yield: 33%. Anal. Calcd for $C_{202}H_{112}F_{72}N_{12}O_{24}P_4Pt_2Yb_4$: C, 42.83; H, 1.99; N, 2.97. Found: C, 43.15; H, 2.14; N, 2.93. IR (KBr, cm^{-1}): ν 2099 m (C≡C), 1658 s (C═O).

Crystal Structure Determination. Crystals of **1**, **6**, **7**, and **9** suitable for X-ray diffraction studies were obtained by layering *n*-hexane onto the dichloromethane solutions. Single crystals sealed in capillaries with mother liquors were measured on a Rigaku Mercury CCD diffractometer by ω scan technique at room temperature with graphite-monochromated Mo Kα radiation (λ = 0.710 73 Å). The CrystalClear software package was used for data reduction and empirical absorption correction. The structures were solved by direct method. The heavy atoms were located from the *E*-map, and the rest of the non-hydrogen atoms were found in subsequent Fourier maps. Most of the non-hydrogen atoms were refined anisotropically except for some disordered F atoms, whereas the hydrogen atoms were generated geometrically with isotropic thermal parameters. The structures were refined on F^2 by full-matrix least-squares methods using the SHELXTL-97 program package.[24] For some disordered $-CF_3$ groups, restrained refinements were carried out by fixing the C−F distances at 1.31 Å with the occupancy factors of a pair of the corresponding F atoms being 0.50, respectively. The crystallographic data for **1**·2CH_2Cl_2·H_2O, **6**, **7**, and **9**·2CH_2Cl_2 are summarized in Table 1.

(24) Sheldrick, G. M. *SHELXL-97, Program for the Refinement of Crystal Structures*; University of Göttingen: Göttingen, Germany, 1997.

Scheme 1. Synthetic Routes to **1**−**9**

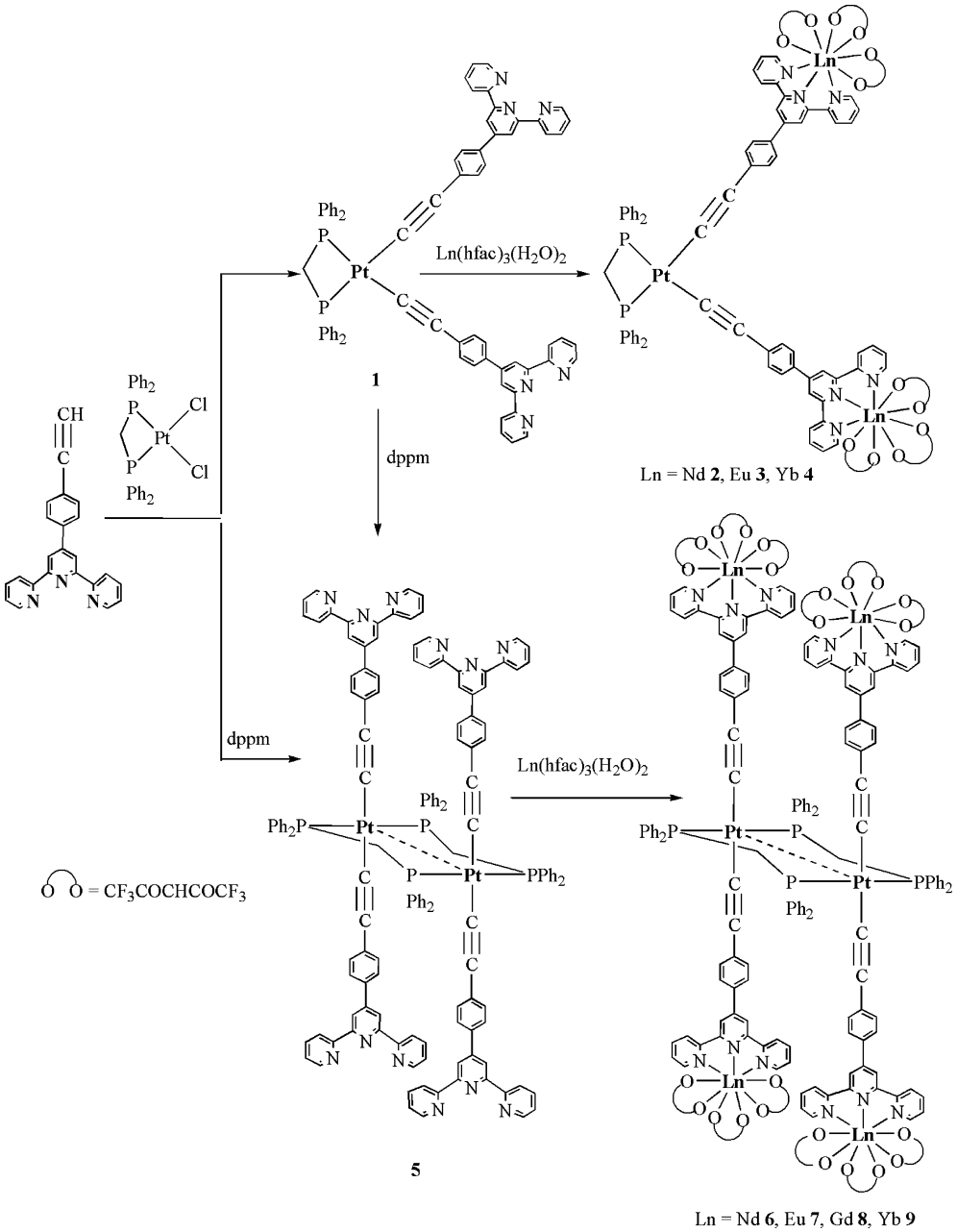

Physical Measurements. UV−vis absorption spectra were measured on a Perkin-Elmer Lambda 25 UV−vis spectrophotometer. Infrared (IR) spectra were recorded on a Magna750 FT-IR spectrophotometer with KBr pellet. Elemental analyses (C, H, N) were carried out on a Perkin-Elmer model 240C elemental analyzer. Electrospray mass spectra (ES-MS) were performed on a Finnigan LCQ mass spectrometer using dichloromethane−methanol mixtures as mobile phases. Emission and excitation spectra in the UV−vis region were recorded on a Perkin-Elmer LS 55 luminescence spectrometer with a red-sensitive photomultiplier type R928. Emission lifetimes in solid states and degassed solutions were determined on an Edinburgh analytical instrument (F900 fluorescence spectrometer) using an LED laser at 397 nm excitation, and the resulting emission was detected by a thermoelectrically cooled Hamamatsu R3809 photomultiplier tube. The instrument response function at the excitation wavelength was deconvolved from the luminescence decay. Near-infrared (NIR) emission spectra were measured on an Edinburgh FLS920 fluorescence spectrometer equipped with a Hamamatsu R5509-72 supercooled photomultiplier tube at 193 K and a TM300 emission monochromator with NIR grating blazed at 1000 nm. The NIR emission spectra were corrected via a calibration curve supplied with the instrument. The emission quantum yields (Φ) of **1**, **3**, **5**, and **7** in degassed dichloromethane solutions at room temperature were calculated by $\Phi_s = \Phi_r(B_r/B_s)(n_s/n_r)^2(D_s/D_r)$ using $[Ru(bpy)_3](PF_6)_2$ in acetonitrile as the standard ($\Phi_{em} = 0.062$), where the subscripts r and s denote reference standard and the sample solution, respectively, and n, D, and Φ are the refractive index of the solvents, the integrated intensity, and the luminescence quantum yield, respectively.[25,26] The quantity B is calculated by $B = 1 - 10^{-AL}$, where A is the absorbance at the excitation wavelength and L is the optical path length. All the solutions used for determination of emission lifetimes and quantum yields were prepared under vacuum in a 10 cm^3 round-bottom flask

(25) Demas, J. N.; Crosby, G. A. *J. Phys. Chem*. **1971**, *75*, 991.
(26) Chan, S. C.; Chan, M. C. W.; Wang, Y.; Che, C. M.; Cheung, K. K.; Zhu, N. *Chem.—Eur. J.* **2001**, *7*, 4180.

Table 2. Selected Bond Distances (Å) and Angles (deg) for **1**, **6**, **7**, and **9**

1		**6**		**7**		**9**	
		Pt···Pt	3.410	Pt···Pt	3.295	Pt···Pt	3.311
Pt−P1	2.268(1)	Pt−P1	2.298(3)	Pt−P1	2.303(3)	Pt−P1	2.288(3)
Pt−C23	2.028(5)	Pt−P2	2.302(3)	Pt−P2	2.309(3)	Pt−P2	2.303(3)
C22−C23	1.183(6)	Pt−C23	2.014(8)	Pt−C23	2.026(9)	Pt−C23	2.004(8)
C36−P1	1.850(3)	Pt−C46	2.005(8)	Pt−C46	1.976(10)	Pt−C46	1.966(8)
Pt−C23−C22	171.9(4)	C22−C23	1.178(12)	C22−C23	1.209(12)	C22−C23	1.197(11)
C23−C22−C19	179.2(6)	C45−C46	1.197(12)	C45−C46	1.207(13)	C45−C46	1.214(11)
C23−Pt−P1	168.9(1)	Nd1−O1	2.518(7)	Eu1−O1	2.446(9)	Yb1−O1	2.396(7)
C23−Pt−P1A	94.99(13)	Nd1−O2	2.436(8)	Eu1−O2	2.425(8)	Yb1−O2	2.329(7)
P1−Pt−P1A	74.13(6)	Nd1−O3	2.443(8)	Eu1−O3	2.433(8)	Yb1−O3	2.394(7)
C23−Pt−C23A	95.9(3)	Nd1−O4	2.441(9)	Eu1−O4	2.413(8)	Yb1−O4	2.329(7)
C22−C23−Pt	171.9(4)	Nd1−O5	2.445(9)	Eu1−O5	2.377(7)	Yb1−O5	2.286(6)
		Nd1−O6	2.423(8)	Eu1−O6	2.371(7)	Yb1−O6	2.283(5)
		Nd1−N1	2.638(10)	Eu1−N1	2.553(9)	Yb1−N1	2.489(7)
		Nd1−N2	2.637(7)	Eu1−N2	2.588(7)	Yb1−N2	2.463(6)
		Nd1−N3	2.603(9)	Eu1−N3	2.590(9)	Yb1−N3	2.493(7)
		C46−Pt−C23	167.5(4)	C46−Pt−C23	167.9(5)	C46−Pt−C23	168.2(4)
		C46−Pt−P1	83.8(3)	C46−Pt−P1	88.9(3)	C46−Pt−P1	89.2(3)
		C23−Pt−P1	90.3(3)	C23−Pt−P1	84.7(3)	C23−Pt−P1	84.4(3)
		C46−Pt−P2	95.5(3)	C46−Pt−P2	92.1(3)	C46−Pt−P2	91.8(3)
		C23−Pt−P2	91.3(3)	C23−Pt−P2	94.7(3)	C23−Pt−P2	95.2(3)
		P1−Pt−P2	175.04(9)	P1−Pt−P2	177.67(11)	P1−Pt−P2	176.93(10)
		C45−C46−Pt	169.4(8)	C45−C46−Pt	173.9(11)	C45−C46−Pt	171.1(9)

equipped with a side arm 1 cm fluorescence cuvette and sealed from the atmosphere by a quick-release Teflon stopper. Solutions used for luminescence determination were prepared after rigorous removal of oxygen by three successive freeze−pump−thaw cycles.

Results and Discussion

Syntheses and Characterization. To the best of our knowledge, reactions of Pt(dppm-*P*,*P*′)Cl_2 with alkynyl ligands always induce isolation of dppm-linked diplatinum(II) complexes $Pt_2(\mu\text{-dppm})_2(C{\equiv}CR)_4$ (R = alkyl or aryl) which have been confirmed by X-ray crystallography for many times.[15,20,21] The mononuclear platinum(II) species Pt(dppm-*P*,*P*′)$(C{\equiv}CR)_2$ (R = alkyl or aryl), however, have never been isolated from these reactions before. Interestingly, when Pt(dppm-*P*,*P*′)Cl_2 reacts with 2.3 equiv of HC≡CPhtpy in the presence of CuI and $^iPr_2NH$, mononuclear platinum(II) complex, c*is*-Pt(dppm-*P*,*P*′)$(C{\equiv}CPhtpy)_2$ (**1**) has been isolated and characterized by X-ray crystallography (vide infra) (Scheme 1). The face-to-face arranged diplatinum(II) complex **5**, however, is inaccessible by the general procedures.[20,21] Instead, **5** has been prepared in a considerably high yield (ca. 59%) by reaction of **1** with 1 equiv of dppm (method A). Alternately, it is also accessible in a low yield (ca. 10%) by reaction of Pt(dppm-*P*,*P*′)Cl_2 with 2.3 equiv of HC≡CPhtpy in the presence of 1 equiv of dppm (method B). It was previously suggested that reactions of Pt(dppm-*P*,*P*′)Cl_2 with excess of dppm ligands induce isolation of mononuclear species *trans*-[Pt(dppm-*P*)$_2(C{\equiv}CR)_2$] containing monodentate coordinated η^1-dppm.[20] The successful isolation of mononuclear platinum(II) species **1** with chelated η^2-dppm is reported for the first time. Due to the poor solubility, both **1** and **5** were isolated by filtration and purified by washing with dichloromethane to remove excess ligands and other impurities.

Reactions of **1** or **5** with excess of $Ln(hfac)_3(H_2O)_2$ (2.5 equiv for **1** and 4.5 equiv for **5**) in dichloromethane afforded heterotrinuclear $PtLn_2$ adducts **(2−4)** or heterohexanuclear Pt_2Ln_4 complexes **(6−9)**. Upon formation of the Pt−Ln heteronuclear adducts, the solubility improved significantly so that the $PtLn_2$ or Pt_2Ln_4 species could be readily purified through recrystallization by layering hexane onto the concentrated dichloromethane solutions. The IR spectra of **1**−**9** exhibit C≡C stretching frequencies at ca. 2100 cm^{-1}, characteristic for Pt−acetylides σ-bonding.[15,20,21] The occurrence of typical ν(C═O) bands at ca. 1655 cm^{-1} demonstrates unambiguously the incorporation of $Ln(hfac)_3$ units with **1** or **5** in the heteronuclear $PtLn_2$ (**2**−**4**) and Pt_2Ln_4 (**6**−**9**) complexes.

Crystal Structures. The structures of **1**, **6**, **7**, and **9** were determined by X-ray crystallography. Selected bond lengths and angles are presented in Table 2. ORTEP drawings of **1** and **6** are depicted in Figures 1 and 2, respectively, and those of **7** and **9** are illustrated in Figures S1 and S2 (Supporting Information).

The Pt^{II} center in **1** adopts a distorted square-planar geometry composed of cis-oriented C_2P_2 donors from σ-coordinated acetylides and chelated dppm. The sum of the angles around the Pt^{II} center is 360°, and the mean deviation of the PtC_2P_2 atoms from the least-squares plane is 0.028

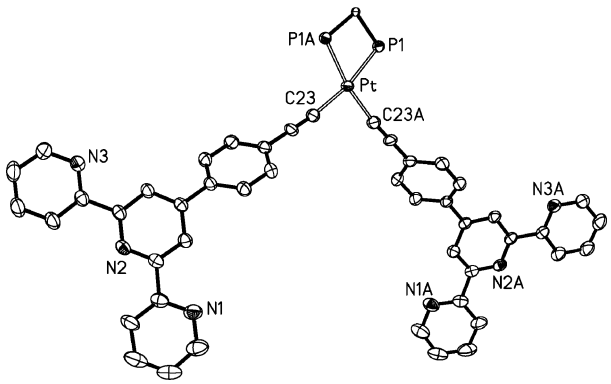

Figure 1. ORTEP drawing of **1** with atom-labeling scheme showing 30% thermal ellipsoids. Phenyl rings on the phosphorus atoms are omitted for clarity.

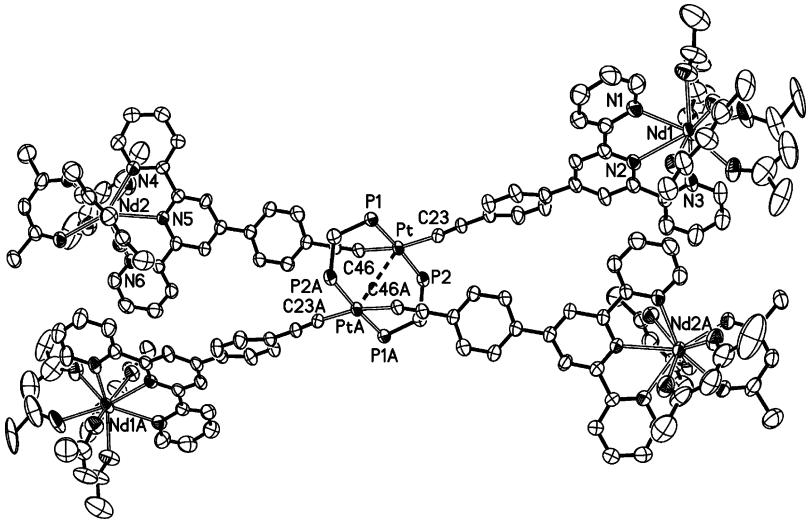

Figure 2. ORTEP drawing of **6** with atom-labeling scheme showing 30% thermal ellipsoids. Phenyl rings on the phosphorus atoms and the F atoms in $-CF_3$ are omitted for clarity.

Å, revealing an excellent coplanarity. The P−Pt−P angle of **1** (74.1(1)°) is much smaller than that of *cis*-Pt(dppe)-(C≡Cphtpy)$_2$ (86.69(6)°)[17] due to the larger constraint in the four-membered PtP_2C ring for **1**. The Pt−C≡C−C array is quasi-linear with Pt−C23−C22 = 171.9(4)° and C23−C22−C19 = 179.2(6)°. The Pt−P (2.268(1) Å) and Pt−C (2.028-(5) Å) distances are comparable to those in Pt(dppe)-(C≡Cphtpy)$_2$ and other Pt−acetylide−dppe analogues.[17−19] The phenyl ring in the C≡CPhtpy forms a dihedral angle of 61.4° with the Pt^{II} coordination plane defined by C_2P_2 donors. Within the C≡CPhtpy ligand, the phenyl and three pyridyl rings are non-coplanar so as to give a dihedral angle of 38.3° formed by the phenyl and the middle pyridyl rings. Furthermore, the middle pyridyl ring forms dihedral angles of 14.1 and 3.6° with the pyridyl rings on two sides, respectively, indicating a great flexibility of the C≡Cphtpy ligand. Intermolecular Pt−Pt contact is absent since the shortest Pt···Pt distance is 10.88 Å between adjacent Pt^{II} atoms in the crystal lattice.

For Pt_2Ln_4 species **6**, **7**, and **9**, the diplatinum(II) $Pt_2(\mu$-dppm)$_2$(C≡CPhtpy)$_4$ subunit exhibits a face-to-face conformations, in which the two Pt^{II} coordination planes are parallelly oriented.[15,20,21] The diplatinum(II) centers are doubly linked by two μ-dppm to give a eight-membered ring consisting of $Pt_2P_4C_2$ atoms. The Pt^{II} atoms are located at distorted square-planar environments built by trans-arranged C_2P_2 donors. The Pt−C and Pt−P distances are comparable to those in **1**. The P1−Pt−P2 angles (175.0(1)−177.7(1)°) are quasi-linear, whereas the C23−Pt−C46 angles (167.5-(4)−168.2(4)°) show some deviation from linearity. The C≡CPhtpy serves as a bifunctional bridging ligand bound to the Pt^{II} centers via Pt−acetylide σ-coordination as well as chelating the Ln^{III} centers through tridentate N_3 donors from the terpyridyl.[17] The intramolecular Pt−Pt distances are 3.41, 3.30, and 3.31 Å in **6**, **7**, and **9**, respectively, comparable to those found in other $Pt_2(\mu$-dppm)$_2$(C≡CR)$_4$ subunit-containing species.[15,20,21] These Pt−Pt distances are shorter than 3.5 Å,[27] which is the upper limit for a significant Pt−Pt interaction. Upon formation of the Pt_2Ln_4 arrays from the diplatinum(II) precursor **5**, the electron density on the diplatinum(II) centers is reduced because of introducing the electron-accepting lanthanide(III) centers, which would probably promote formation of the stronger intramolecular Pt−Pt contacts to compensate for the loss of electron density.[21] The increased bulk in the Pt_2Ln_4 adducts compared with that in **5** would also cause a larger bending for the C−Pt−C bonds, which also pull the platinum atoms into close proximity.[21]

Table 3. UV−Vis Absorption Data for **1**−**9**

compd	λ/nm (ϵ/M^{-1} cm^{-1})
1	233 (93 080), 255 (59 120), 290 (66 800), 328 (70 640), 355 (5200)
2	235 (94 280), 288 (90 550), 306 (98 590), 368 (66 200)
3	235 (90 920), 288 (90 570), 306 (93 310), 367 (64 540)
4	233 (97 570), 288 (108 700), 305 (107 000), 368 (64 920)
5	229 (238 400), 279 (145 200), 352 (115 000), 397 (90 980)
6	289 (225 000), 309 (246 300), 412 (129 000)
7	289 (217 800), 307 (224 500), 412 (113 400)
8	290 (202 400), 306 (214 600), 409 (106 000)
9	290 (242 400), 305 (249 900), 411 (116 500)

The Ln^{III} ions in **6**, **7**, and **9** are nine-coordinated with N_3O_6 donors to afford distorted capped square antiprisms as found in {Pt(dppp)(C≡CPhtpy)$_2$}{Ln(hfac)$_3$}$_2$ (Ln=Eu, Yb).[17] The average Yb−N (2.48 Å) and Yb−O distances (2.33 Å) in **9** are comparable to those in {Pt(dppp)(C≡CPhtpy)$_2$}-{Yb(hfac)$_3$}$_2$.[17] The intramolecular Pt···Ln distances across the bridging C≡CPhtpy are 14.32 and 14.09 Å in **6**, 14.13 and 14.15 Å in **7**, and 14.01 and 14.08 Å in **9**, respectively. The dihedral angles formed by the phenyl and the middle pyridyl in the C≡CPhtpy are 25.1 and 24.6° for **6**, 12.1 and 25.4° for **7**, 7.1 and 22.5° for **9**, revealing that the bridging C≡CPhtpy displays a better coplanarity in the Pt_2Ln_4 arrays compared with that in **1** (38.3°).

UV−Vis Absorption Properties. UV−vis absorption data for **1**−**9** in dichloromethane solutions at 298 K are summarized in Table 3. For the purpose of comparison, the UV−vis spectra of mononuclear species **1** and face-to-face

(27) Field, J. S.; Gertenbach, J.-A.; Haines, R. J.; Ledwaba, L. P.; Mashapa, N. T.; McMillin, D. R.; Munro, O. Q.; Summerton, G. C. *Dalton Trans.* **2003**, 1176.

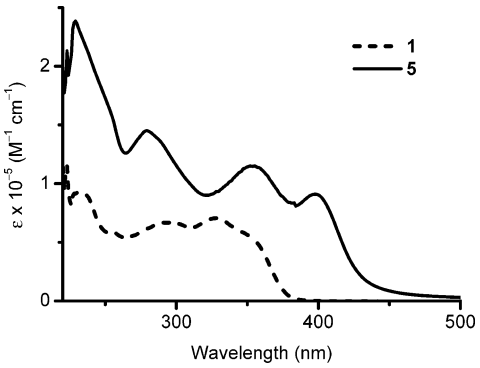

Figure 3. UV−vis absorption spectra of **1** and **5** in dichloromethane solutions at room temperature.

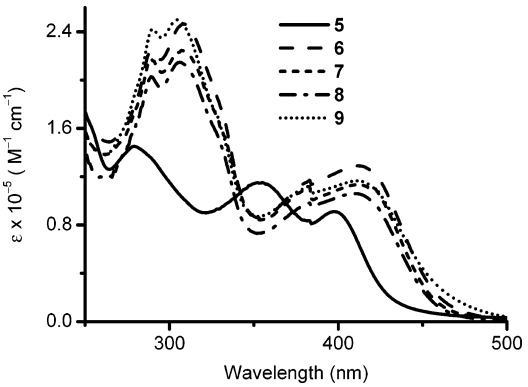

Figure 4. UV−vis absorption spectra of **5**−**9** in dichloromethane solutions.

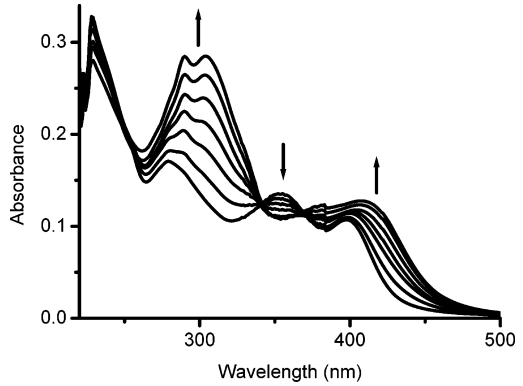

Figure 5. Changes in the UV−vis absorption spectra by titration of **5** with $Yb(hfac)_3(H_2O)_2$ in dichloromethane solutions.

arranged diplatinum(II) complex **5** are shown in Figure 3. The electronic absorption spectra of $PtLn_2$ (**2**−**4**) and Pt_2Ln_4 (**6**−**9**) species along with their precursors **1** or **5** are depicted in Figure S3 (Supporting Information) and Figure 4, respectively.

The UV−vis spectrum of **1** exhibits high-energy bands at 230−260 nm due to dppm-centered transitions and absorption at ca. 280−328 nm induced likely by $\pi \rightarrow \pi^*$ transitions of the C≡Cphtpy. By analogy with the corresponding absorptions in $Pt(dppe)(C{\equiv}Cphtpy)_2$,[17] $Pt(dppp)(C{\equiv}Cphtpy)_2$,[17] and *trans*-$Pt(dppm\text{-}P)_2(C{\equiv}CR)_2$ (R = C_6H_4Me-*p*, Ph, CH_2CH_2Ph, or $C(Me){=}CH_2$),[20] the lower energy absorption shoulder at ca. 355 nm tailing to ca. 400 nm is tentatively ascribed to metal-perturbed $\pi \rightarrow \pi^*$ (C≡C) transitions in the C≡CPhtpy, mixed probably with some d(Pt) → π^*(C≡CPhtpy) MLCT (metal-to-ligand charge transfer) character.[17]

The diplatinum(II) species **5** exhibits two intense low-energy absorptions at ca. 352 and 397 nm in dichloromethane solution. By comparison with the corresponding low-energy absorptions in **1**, *trans*-$Pt(dppm\text{-}P)_2(C{\equiv}CR)_2$ (R = C_6H_4Me-*p*, Ph),[20] other face-to-face arranged diplatinum(II) complexes $Pt_2(\mu\text{-}dppm)_2(C{\equiv}CR)_4$ (R = alkyl or aryl),[15,21] and "A-frame" type diplatinum(II) complexes,[28,29] the intense absorption at 352 nm is ascribable to [d(Pt) → π^*(C≡CPhtpy)] MLCT transition mixed probably with some $\pi \rightarrow \pi^*$ character in the C≡CPhtpy, whereas that at ca. 397 nm originates likely from spin-allowed [$d_\sigma^*(Pt_2) \rightarrow p_\sigma(Pt_2)$/$\pi^*$(C≡CPhtpy)] MMLCT (metal−metal-to-ligand charge transfer) states as described previously by Yam et al.[21b,d] Compared with that in **1**, the low-energy MLCT absorption in **5** is strikingly intensified in addition to occurrence of another strong absorption with a lower energy due to MMLCT state as indicated in Figure 3. Therefore, the structural difference between **1** and **5** is unambiguously reflected in the strikingly different UV−vis absorption character.

As shown in Figure S3 (Supporting Information) and Figure 4, compared with those in the precursors **1** or **5**, the corresponding low-energy absorptions exhibit distinctly red shifts (10−15 nm) in the $PtLn_2$ and Pt_2Ln_4 heteronuclear complexes besides the appearance of a new absorption band at ca. 305 nm arising from the $Ln(hfac)_3$ units. Incorporation of $Ln(hfac)_3$ with **1** or **5** via terpyridyl chelation in the bridging C≡CPhtpy causes a reduction of the LUMO energy and a reduced energy gap between HOMO (dπ (Pt)) and LUMO (π^*(C≡CPhtpy)), thus resulting in an obviously red-shifted character for the MLCT or/and MMLCT absorptions in the $PtLn_2$ and Pt_2Ln_4 complexes.[15−17] Addition of $Ln(hfac)_3(H_2O)_2$ to a dichloromethane solution of **1** or **5** results gradually in a deepening of the color from pale yellow to yellow, which is associated with the enhanced and red-shifted MLCT absorption upon formation of the $PtLn_2$ or Pt_2Ln_4 arrays, as indicated by the change of the UV−vis absorption spectra upon titration of **1** (Figure S4, Supporting Information) with $Nd(hfac)_3(H_2O)_2$ or titration of **5** with $Yb(hfac)_3(H_2O)_2$ (Figure 5) in dichloromethane solutions. Figure S5 (Supporting Information) shows the changes of the absorbance at 367 nm in the titration of **1** with $Nd(hfac)_3(H_2O)_2$ versus the ratio of Nd^{III} to Pt^{II}, fitting well to a 2:1 binding ratio between Nd and Pt moieties.

Luminescence Properties. The emission spectra of **1** and **5** in dichloromethane solutions at room temperature are illustrated in Figure 6. The luminescence data for these complexes are collected in Table 4. Upon irradiation at λ_{ex} = 250−390 nm, the solid sample of **1** exhibits a weak, short-lived, high-energy emission at ca. 423 nm (τ < 1 ns) and a long-lived, low-energy emission at 558 nm (τ = 10.2 μs).

(28) Yam, V. W. W.; Chan, L. P.; Lai, T. F. *Organometallics* **1993**, *12*, 2197.
(29) Yam, V. W. W.; Yeung, P. K. Y.; Chan, L. P.; Kwok, W. M.; Phillips, D. L.; Yu, K. L.; Wong, R. W. K.; Yan, H.; Meng, Q. J. *Organometallics* **1998**, *17*, 2590.

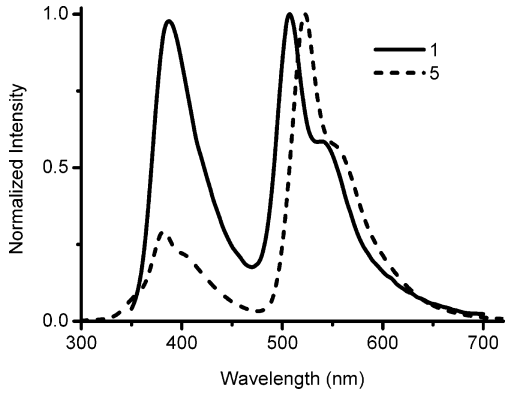

Figure 6. Emission spectra of **1** and **5** in fluid dichloromethane solutions at room temperature.

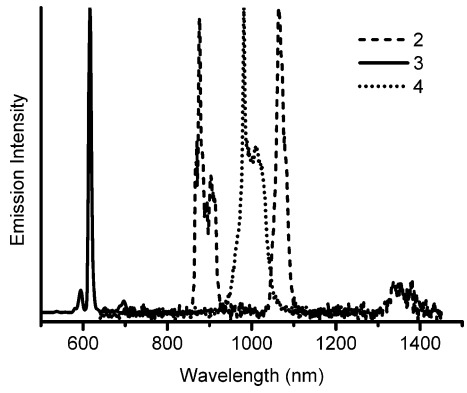

Figure 7. Lanthanide emission spectra of **2**−**4** in dichloromethane solutions.

Table 4. Luminescence Data for **1**−**9** at 298 K

compd	λ_{em}/nm (τ_{em}/μs) (solid)	λ_{em}/nm (τ_{em}/μs) (CH_2Cl_2)	Φ (%)[a,b]
1	423 (<1 ns)	388 (<1 ns)	0.18[a] (Φ_F)
	496 sh, 558 (10.2)	508 (0.17), 542 sh	0.16[a] (Φ_P)
2	1060 (weak)	1060 (weak)	
3	615 (652.3)	615 (1027)	3.73[a]
4	980 (14.78)	980 (15.9)	0.80[b]
5	524 (6.5), 559 sh	382 (<1 ns)	1.33[a] (Φ_F)
		523 (9.4), 559 sh	3.26[a] (Φ_P)
6	1060 (weak)	1060 (weak)	
7	615 (549.9)	615 (442.7)	1.20[a]
8		461, 610 sh (1.39), 661	
9	980 (16.43)	980 (15.48)	0.77[b]

[a] The quantum yields of complexes **1**, **3**, **5**, and **7** in degassed CH_2Cl_2 are determined relative to that of $[Ru(bpy)_3](PF_6)_2$ ($\Phi = 0.062$) in degassed CH_3CN.[17,34,35] [b] The quantum yields of Yb^{III} complexes in dichloromethane solution are estimated by the equation $\Phi = \tau_{obs}/\tau_0$, in which τ_{obs} is the observed emission lifetime and τ_0 is the radiative or "natural" lifetime with 2 ms.

The vibronic progression spacing of the low-energy emission is 2240 cm^{-1}, which is typical of the ν(C≡C) frequency in the acetylides. In degassed dichloromethane solution at 298 K, **1** also shows a short-lived (τ < 1 ns), intense emission at ca. 388 nm and a relatively long-lived ($\tau = 0.17$ μs) intense emission at ca. 508 nm. The vibronic progression spacing of the low-energy emission is 1269 cm^{-1}, which is typical of the ν(C⋯C) and ν(C⋯N) aromatic vibrational modes in the C≡CPhtpy ligands.[17] In contrast with the large Stokes' shifts (8480 cm^{-1}) for the low-energy emission ($\lambda_{em} = 508$ nm) in fluid dichloromethane solution, the high-energy emission ($\lambda_{em} = 388$ nm) displays much smaller Stokes' shift (4715 cm^{-1}). Consequently, the short lifetime together with small Stokes' shift suggests that the high-energy emission is derived from $^1[\pi \rightarrow \pi^*]$ (C≡CPhtpy) intraligand (^{1}ILCT) fluorescence, whereas the large Stokes' shift and long-lived lifetime reveal that the low-energy emission arises probably from ^{3}[d(Pt) → π^*(C≡CPhtpy)] (^{3}MLCT) transition, mixed with some $^3[\pi \rightarrow \pi^*]$ (C≡CPhtpy) (^{3}ILCT) triplet excited states.[17,30] With excitation at $\lambda_{ex} = 250-450$ nm, **5** emits an intense, long-lived luminescence at ca. 524 nm in both solid state and fluid dichloromethane solution, assignable to $^3[d_\sigma^*(Pt_2) \rightarrow p_\sigma(Pt_2)/\pi^*$(C≡CPhtpy)] (^{3}MMLCT) phosphorescence as that in other face-to-face diplatinum(II) species $Pt_2(\mu\text{-dppm})_2(C{\equiv}CR)_4$ (R = alkyl or aryl).[15,21] In addition, with excitation at $\lambda_{ex} = 250-320$ nm, a short-lived (τ < 1 ns), high-energy emission due to ^{1}ILCT (C≡CPhtpy) transition is also observed at ca. 382 nm in fluid dichloromethane solution of **5**.

Upon excitation at $\lambda_{ex} = 360-450$ nm (**2**−**4**) or 360−500 nm (**6**, **7**, and **9**) which is the absorption region of Pt^{II} alkynyl chromophores, the $PtLn_2$ (**2**−**4**) or Pt_2Ln_4 (**6**, **7**, and **9**) complexes exhibit characteristic luminescence of the corresponding Ln^{III} ions in both solid states and dichloromethane solutions, demonstrating unambiguously that sensitized lanthanide luminescence is indeed achieved by $Pt^{II} \rightarrow Ln^{III}$ (Ln = Nd, Eu, Yb) energy transfer from the Pt^{II}-based MLCT or MMLCT excited triplet state because the model complex Ln(hfac)$_3$(HC≡CPhtpy) lacks of obvious absorption at λ > 360 nm (Figure S6, Supporting Information). The typical Ln^{III} emission spectra of **2** (Nd), **3** (Eu), and **4** (Yb) in dichloromethane solutions are illustrated in Figure 7. As expected, five emission bands were observed for Eu species at ca. 581 ($^5D_0 \rightarrow F_0$), 595 ($^5D_0 \rightarrow {}^7F_1$), 615 ($^5D_0 \rightarrow {}^7F_2$), 652 ($^5D_0 \rightarrow {}^7F_3$), and 696 nm ($^5D_0 \rightarrow {}^7F_4$), three were found for Nd species at ca. 877 ($^4F_{3/2} \rightarrow {}^4I_{9/2}$), 1060 ($^4F_{3/2} \rightarrow {}^4I_{11/2}$), and 1335 nm ($^4F_{3/2} \rightarrow {}^4I_{13/2}$), and one was found for Yb species at ca. 980 nm ($^2F_{5/2} \rightarrow {}^2F_{7/2}$).

In addition to the lanthanide luminescence, moderate high-energy emission at 430−470 nm is observed in fluid dichloromethane solutions of the $PtLn_2$ and Pt_2Ln_4 species (Figure S7, Supporting Information) owing probably to the red-shifted ^{1}ILCT fluorescence from the $^1[\pi \rightarrow \pi^*]$ excited state of C≡Cphtpy. For the $PtLn_2$ species, since the tail of the ^{1}ILCT fluorescence emission may superpose with the phosphorescence from ^{3}ILCT state in the Pt(C≡Cphtpy)$_2$ moiety, it is uncertain whether the phosphorescence of the Pt^{II} alkynyl chromophore is entirely quenched or not.[17] For the Pt_2Gd_4 species **8**, upon excitation at $\lambda_{ex} = 250-500$ nm, a moderate emission at 660 nm occurs in dichloromethane solution, which is likely ascribed to the Pt^{II} alkynyl-based phosphorescence (Figure S7, Supporting Information). For other Pt_2Ln_4 (Ln = Nd (**6**), Eu (**7**), Yb (**9**)) species, weak emission at ca. 610 nm (Figure S7, Supporting Information) is also observed, which is likely the residual Pt^{II} alkynyl-based ^{3}MMLCT phosphorescence (Ln = Nd, Eu, Yb), implying that Pt → Ln energy transfer from the Pt^{II}-based

(30) Emmert, L. A.; Choi, W.; Marshall, J. A.; Yang, J.; Meyer, L. A.; Brozik, J. A. *J. Phys. Chem. A* **2003**, *107*, 11340.

antenna donors to the Ln^{III} centers (Ln = Nd, Eu, Yb) is incomplete. Noticeably, the low-energy emission (610−660 nm) from the ^{3}MMLCT state is highly red-shifted compared with that in the diplatinum(II) precursor **5** (523 nm), ascribable perhaps to the enhanced Pt−Pt contacts upon formation of the Pt_2Ln_4 arrays, inducing a reduced energy gap between HOMO and LUMO and thus a red-shifted ^{3}MMLCT absorption.[21]

When the residual phosphorescence from the Pt^{II} alkynyl chromophores was monitored at 610 nm, the lifetimes of unquenched Pt-based emission are 4.1 ns for Pt_2Nd_4 (**6**), 1390 ns for Pt_2Gd_4 (**8**), and 637 ns for Pt_2Yb_4 (**9**) species in fluid dichloromethane at room temperature. Taking into account the statistical factor, the rates k_{ET} of Pt → Ln energy transfer from the diplatinum(II) chromophores $Pt_2(\mu\text{-dppm})_2(C{\equiv}CPhtpy)_4$ to the lanthanide ions can thus be evaluated by the equation $k_{ET} = (1/\tau - 1/\tau_0)/4$,[4−7,15a] where τ is the lifetime of residual Pt-based emission in the Pt_2Ln_4 (Ln = Nd (**6**), Yb (**9**)) species and τ_0 (1.39 μs) is the lifetime in the reference Pt_2Gd_4 (**8**) complex which cannot accept any energy from the Pt^{II}-based antenna triplet states because Gd^{III} has no energy levels below 32 000 cm^{-1}. Since the luminescence lifetime of Pt_2Gd_4 (**8**) species can be regarded as the ^{3}MMLCT state lifetime in the absence of Pt → Ln energy transfer,[4] the energy transfer rates (k_{ET}) can thus be calculated as $k_{ET} = (1/\tau_{PtNd} - 1/\tau_{PtGd})/4 = 6.07 \times 10^7\ s^{-1}$ for Pt_2Nd_4 (**6**) and $k_{ET} = (1/\tau_{PtYb} - 1/\tau_{PtGd})/4 = 2.12 \times 10^5\ s^{-1}$ for Pt_2Yb_4 (**9**) species. Obviously, the k_{ET} values indicate that Pt → Ln energy transfer in these species is much slower than that in the Pt_2Ln_2 or Pt_2Ln_4 complexes (complete energy transfer) across bridging 2,2′-bipyridine-5-acetylide or 1,10-phenanthroline-5-acetylide with Pt···Ln being 8.0−10.5 Å[15b] but faster than those in the Pt_6Ln_6 ($k_{ET} = 1.02 \times 10^7\ s^{-1}$ for Pt_6Nd_6 and $k_{ET} = 1.83 \times 10^5\ s^{-1}$ for Pt_6Yb_6) species with Pt···Ln being 10.5−16.7 Å.[15a] The faster Pt → Ln energy transfer for Pt_2Nd_4 (**6**) complex than that for Pt_2Yb_4 (**9**) species can be rationalized by the better spectroscopic overlap between the emission spectrum of the Pt^{II} alkynyl-based antenna chromophore and the absorption spectrum of the Nd^{III} ion.[1,4−7] For Yb^{III} ion, a single f−f absorption at ca. 980 nm (10 240 cm^{-1}) can only overlap with the very weak low-energy tail of the Pt^{II}-based emission. Nd^{III} ion, however, has 10 f−f levels lying within 11 000−20 000 cm^{-1} (910−500 nm), which affords much better energy match with the Pt^{II} alkynyl-based triplet states.

In view of the conjugated character of the C≡CPhtpy ligands as well as the favorable spectral overlapping between the emission of Pt^{II}-based donor and the f−f absorptions of Ln(III) acceptors in the relevant region, the energy transfer process is probably related to an electron-exchange mechanism (Dexter-type transfer through bond). Alternately, the intramolecular Pt···Ln distance is ca. 14.2 Å across the bridging C≡CPhtpy, which is favorable to dipole−dipole energy transfer (Förster-type transfer through space). When Ln = Eu^{III} or Nd^{III}, the transitions follow both the selection rules for Dexter ($|\Delta J| = 0$ or 1) (with the exception of $J = J' = 0$, which is forbidden) and Förster types ($|\Delta J| = 2$, 4, or 6).[5d] When Ln = Yb^{III}, since only one possible transition ($^2F_{7/2} \rightarrow {}^2F_{5/2}$) is present for the Yb^{III} ion, Dexter-type energy transfer is most likely operating.[5d,16]

Summary

In contrast with the general isolation of face-to-face diplatinum(II) species $Pt_2(\mu\text{-dppm})_2(C{\equiv}CR)_4$ (R = alkyl or aryl) by reaction of Pt(dppm-P,P′)Cl_2 with HC≡CR, mononuclear complex *cis*-Pt(dppm-*P*,*P*′)(C≡CPhtpy)$_2$ (**1**) is unusually accessible from the reaction using HC≡CPhtpy as the alkynyl ligand. **1** can be transformed into face-to-face diplatinum(II) complex $Pt_2(\mu\text{-dppm})_2(C{\equiv}CPhtpy)_4$ (**5**) species by addition of equimolar dppm. Both **1** and **5** exhibit intense, long-lived room-temperature phosphorescence originating from an admixture of ^{3}ILCT [$\pi{\rightarrow}\pi^*$(C≡Cphtpy)] and ^{3}MLCT [d(Pt)π^*(C≡CPhtpy)]/^{3}MMLCT [$d_\sigma{}^*(Pt_2) \rightarrow p_\sigma(Pt_2)/\pi^*$(C≡CPhtpy)] triplet states. The phosphorescent character qualifies **1** and **5** as favorable energy donors to facilitate Pt → Ln energy transfer in the $PtLn_2$ and Pt_2Ln_4 adducts formed by incorporating with $Ln(hfac)_3(H_2O)_2$ via terdentate chelation of terpyridyl in the bridging C≡CPhtpy. With excitation at λ_{ex} = 360−450 ($PtLn_2$) or λ_{ex} = 360−500 nm (Pt_2Ln_4) which is the absorption region of the Pt^{II} alkynyl antenna chromophores, sensitized lanthanide luminescence is successfully achieved in the $PtLn_2$ and Pt_2Ln_4 complexes, demonstrating unambiguously that efficient Pt → Ln energy transfer occurs indeed across the bridging C≡CPhtpy with intramolecular Pt···Ln distances being ca. 14.2 Å.

Acknowledgment. This work was financially supported by the NSFC (Grants 90401005, 20490210, 20521101, and 20625101), the 973 project (Grant 2007CB815304) from MSTC, the NSF of Fujian Province (Grant E0420002), and the Key Project from CAS (Grant KJCX2-YW-H01).

Supporting Information Available: Additional structural drawings (Figures S1 and S2), absorption and emission spectra (Figures S3−S7), and X-ray crystallographic files in CIF format for the structure determinations of **1**, **6**, **7**, and **9**. This material are available free of charge via the Internet at http://pubs.acs.org.

IC7015676